A simple equation of state for the Lennard-Jones fluid

A new reference term for equations of state and perturbation theories

N.K. Koutras, V.I. Harismiadis and D.P. Tassios

Department of Chemical Engineering, National Technical University of Athens, Zographos, 15773 (Greece)

(Received October 22, 1992; accepted in final form February 2, 1992)

ABSTRACT

Koutras, N.K., Harismiadis, V.I. and Tassios, D.P., 1992. A simple equation of state for the Lennard-Jones fluid: a new reference term for equations of state and perturbation theories. *Fluid Phase Equilibria*, 77: 13–38.

A simple equation of state (EoS) for the Lennard-Jones (LJ) fluid that has a form similar to the Carnahan–Starling (CS) equation of state for the hard sphere fluid is presented. Excellent agreement between simulation data and calculated values for vapor pressures, saturated liquid and vapor densities and vapor *PVT* behavior is obtained for subcritical temperatures except in the critical region. For supercritical temperatures, the results are satisfactory but become less so with increased temperature and density. When combined with the van der Waals one fluid theory, the proposed equation provides satisfactory agreement with molecular simulation vapor–liquid equilibria results for binary LJ mixtures. Its overall behavior makes it suitable for use as a reference term in equations of state for real fluids.

INTRODUCTION

The successful application of perturbation theory in describing the behavior of real fluids requires the use of a reference fluid that:

Correspondence to: V.I. Harismiadis. Current address: Koninklijke/Shell-Laboratorium, Amsterdam, ST/2 department, Postbus 3003, 1003 AA Amsterdam-Noord, The Netherlands. E-mail: harismi1@ksla.nl

(1) is close to reality, i.e. it contains the essential features of a real fluid, and

(2) its behavior is well understood.

The most commonly used reference fluid is that of hard spheres, whose *PVT* behavior has been obtained from molecular simulation and is successfully described by the Carnahan–Starling equation of state (1969):

$$z = \frac{1 + y + y^2 - y^3}{(1 - y)^3} \tag{1}$$

$$y = \frac{\pi}{6}\rho\sigma^3 \tag{2}$$

where σ is the hard sphere diameter and ρ is the number density. The hard sphere fluid meets successfully the second requirement for a reference fluid but not the first one, since it involves repulsive forces only. A reference fluid involving attractive forces also would obviously be a much better choice.

Bryan and Prausnitz (1987) developed an equation of state for polar fluids using as a reference term a modification of eqn. (1) which describes dipolar hard spheres:

$$z = \frac{1 + \phi_1 y + \phi_2 y^2 - \phi_3 y^2}{(1 - y)^3} \tag{3}$$

$$\phi_i = 1 + a_i \hat{\mu} + b_i \hat{\mu}^2 + c_i \hat{\mu}^3 + d_i \hat{\mu}^4 \tag{4}$$

$$\hat{\mu} = \sqrt{\frac{\mu}{\sigma^3 kT}} \tag{5}$$

where μ is the dipole moment and the coefficients used in eqn. (4) were chosen to match the Padé approximant developed by Rushbrooke, Stell and Høye for the Helmholtz energy of dipolar hard spheres (Rushbrooke et al., 1973).

A reference fluid of general application could be the Lennard-Jones fluid, described by the following pairwise additive intermolecular potential:

$$U_{ij} = 4\epsilon_{ij}\left[\left(\frac{\sigma_{ij}}{r}\right)^{12} - \left(\frac{\sigma_{ij}}{r}\right)^6\right] \tag{6}$$

where U_{ij} is the interaction energy between one molecule of species i and one of species j at a distance r, while ϵ_{ij} and σ_{ij} are, respectively, a characteristic energy and a characteristic length for the above pair of molecules (energy and size LJ potential parameters for unlike molecular

interactions). It is clear that this potential is a conformal one and that it satisfies the two parameters corresponding states principle.

Although an inaccurate representation of the intermolecular potential even for inert gases, the Lennard-Jones fluid is sufficiently close to reality. In fact, it is one of the simplest potential models that incorporates both attractive and repulsive forces. Thus, it provides a convenient model for testing liquid theories and investigating a variety of fluid behavior phenomena. Equations of state for this fluid are available (Nicolas et al., 1979; Adachi et al., 1988), but they are of a Benedict–Webb–Rubin (BWR) type and their use as a reference term in equations of state for real fluids would be impractical.

It is the purpose of this paper to present a much simpler, Carnahan–Starling-type equation of state for the Lennard-Jones fluid, which describes the following properties:

(1) vapor pressure and saturated liquid volumes;

(2) *PVT* behavior;

(3) second virial coefficients.

The resulting equation of state is tested in this work in the prediction of binary vapor–liquid equilibria (VLE) behavior, using the van der Waals one fluid theory and the recent molecular simulation data of Harismiadis et al. (1991).

PURE LENNARD-JONES FLUID DATA BASE

The Lennard-Jones fluid has been studied by both theoretical and computer simulation methods. The first approach provides values of the reduced virial coefficients (up to the fifth) for the LJ fluid (Barker et al., 1966); the second, *PVT* and VLE (vapor pressures and saturated densities) data.

Nicolas et al. (1979) and later Adachi et al. (1988) present the pure LJ fluid *PVT* data that were known until then, which are mainly on isochores and cover even the unstable and metastable region of the phase diagram.

Pure LJ fluid VLE data are given by various authors and are reproduced in Table 1 in terms of the reduced quantities

$$P^* = \frac{P\sigma^3}{\epsilon} \qquad T^* = \frac{kT}{\epsilon} \qquad \rho^* = \rho\sigma^3 \tag{7}$$

In this work we used simulation vapor pressure and saturated liquid density values for reduced temperatures ranging from the triple point ($T^* = 0.68 \pm 0.02$, Hansen and Verlet, 1969) to the critical point ($T_c^* =$

TABLE 1

Pure LJ fluid VLE data

T^*	ρ_V^*	ρ_L^*	P_s^*	Source [b]
1.30	0.24 (2) [a]	0.45 (3)	0.125 (7)	4
	0.17 (1)	0.47 (3)	0.119 (5)	4
	0.21 (1)	0.46 (3)	0.121 (6)	5
	0.22 (2)	0.43 (2)	0.127	3
	0.20 (5)	0.42 (7)	0.121 (8)	6
1.25	0.123 (14)	0.505 (23)	0.091 (9)	4
	0.110 (17)	0.533 (40)	0.089 (9)	4
	0.152 (15)	0.529 (9)	0.101 (9)	5
	0.148 (3)	0.526 (15)	0.101 (6)	5
	0.19	0.544	0.111	3
1.225	0.105 (8)	0.536 (16)	0.0836 (32)	7
1.20	0.094 (9)	0.563 (16)	0.0749 (42)	7
	0.098 (10)	0.564 (16)	0.076 (4)	6
	0.112 (31)	0.564 (24)	0.079 (7)	6
	0.125 (40)	0.552 (54)	0.070 (9)	6
1.15	0.076 (7)	0.606 (12)	0.061 (7)	4
	0.082 (5)	0.610 (2)	0.064 (4)	4
	0.072 (9)	0.605 (9)	0.059 (3)	5
	0.083 (6)	0.612 (9)	0.064 (5)	5
	0.075 (3)	0.607 (8)	0.062 (3)	6
	0.075 (9)	0.601 (20)	0.056 (7)	6
	0.073	0.606	0.0597	1
	0.0775	0.609	0.0630	3
1.10	0.066 (5)	0.651 (10)	0.0515 (28)	7
	0.0468	0.6319	0.0413	2
1.05	0.045 (3)	0.675 (6)	0.0366 (19)	7
	0.0351	0.67231	0.0310	2
1.00	0.0281 (32)	0.698 (3)	0.0239 (23)	4
	0.0271 (37)	0.695 (5)	0.0233 (27)	4
	0.0283 (6)	0.703 (3)	0.0241 (15)	5
	0.0291 (6)	0.702 (6)	0.0246 (12)	5
	0.0261	0.70298	0.0227	2
0.95	0.0190	0.73044	0.0161	2
0.90	0.0115 (14)	0.753 (7)	0.0096 (1)	4
	0.0151 (3)	0.758 (9)	0.0123 (6)	5
	0.01313	0.75581	0.0108	2
0.85	0.00878	0.77980	0.00701	2
0.80	0.00558	0.80303	0.00427	2

TABLE 1 (continued)

T^*	ρ_V^*	ρ_L^*	P_s^*	Source [b]
0.75	0.0028 (2)	0.820 (6)	0.0019 (2)	4
	0.0027 (4)	0.820 (5)	0.0019 (3)	4
	0.0031 (3)	0.819 (3)	0.0023 (3)	5
	0.0035	0.825	0.0025	1
	0.00331	0.82611	0.00241	3
0.70	0.00182	0.84944	0.00125	2
0.65	0.000896	0.87296	0.000576	2
0.60	0.000385	0.89586	0.000230	2

[a] The numbers given in parentheses are the estimated errors in terms of the last decimal digit presented, e.g. 0.820(6) means 0.820 ± 0.006.
[b] 1, Hansen and Verlet, 1969; 2, Adams, 1976; 3, Adams, 1979; 4, Panagiotopoulos, 1987; 5, Panagiotopoulos et al., 1988; 6, Smit and Frenkel, 1989; 7, Panagiotopoulos, 1991. These simulations were performed with 600 molecules. The Monte Carlo Gibbs method that satisfies the microscopic reversibility (Harismiadis et al., 1991) was used.

1.316 ± 0.006, $P_c^* = 0.13 \pm 0.01$, $\rho_c^* = 0.304 \pm 0.006$ (Smit, 1990; Panagiotopoulos, 1991)) of the LJ fluid.

In view of the generally large scatter of the simulation data and in order to facilitate our calculations, the available vapor pressure, saturated liquid density and second virial coefficient data were first correlated with the reduced temperature.

Vapor pressure correlation

Several expressions for P_s^* as a function of T^* were considered. Best results, with an average absolute deviation of 1.60% in $\ln P_s^*$, were obtained with the Wagner expression (Reid et al., 1987):

$$\ln\left(\frac{P_s^*}{P_c^*}\right) = \frac{aq + bq^{1.5} + cq^3 + dq^6}{1 - q} \tag{8}$$

where q is defined as

$$q = 1 - \frac{T^*}{1.316} \tag{9}$$

The parameter values are given in Table 2. In view of the uncertainty in the experimental P_c^* value, P_c^* in eqn. (8) was treated as an adjustable parameter so that the best agreement with simulation data was obtained. Thus, P_c^* was estimated to be 0.1280.

TABLE 2

Parameter values in the expressions for the correlations of vapor pressure (eqn. (8)), saturated liquid densities (eqn. (10)) and reduced second virial coefficient (eqn. (14)) with the reduced temperature

Parameter	P_s^*	y_L	B_2^*
a	-4.89078	-1.727181	0.403609
b	-1.36238	3.334780	1.45966
c	4.45037	-4.541626	-4.06342
d	-28.1163	2.293716	0.0810159
e	–	0.275536	-0.418404
P_c^*	0.127970	–	–
y_c	–	0.159174	–
Aver. abs. deviation (%)	1.599 (in ln P_s^*)	0.9291	0.1105

Saturated liquid density correlation

Several expressions were evaluated. The best results were obtained using the following modified Hankinson–Brobst–Thomson (Reid et al., 1987) expression:

$$\frac{1}{y_L} = \frac{1}{y_c}(1 + aq + bq^2 + cq^3 + dq^4) \tag{10}$$

where

$$q = \left(1 - \frac{T}{1.316}\right)^e \tag{11}$$

The overall average absolute deviation in y_L is 0.93% and the parameter values are given in Table 2.

Second virial coefficient correlation

The reduced second virial coefficient for the LJ fluid is defined by the expression

$$B_2^* = \frac{1}{b_0} \lim_{\rho \to 0} \left(\frac{\partial z}{\partial \rho}\right) \tag{12}$$

where ρ is the number density and b_0 is given by

$$b_0 = \tfrac{2}{3}\pi\sigma^3 \tag{13}$$

The values of the reduced second virial coefficient were correlated with the reduced temperature using several expressions, including the ones proposed by Abbott (1973), Tsonopoulos (1974) and Daubert and Danner (1989) for the temperature dependence of real fluids' second virial coefficients. The best results were obtained using the expression

$$B_2^* = a + \frac{b}{\sqrt{T^*}} + \frac{c}{T^*} + \frac{d}{T^{*2}} + \frac{e}{T^{*3}} \tag{14}$$

which has the same form as that obtained for the B_2^* from the Nicolas et al. BWR equation of state for the LJ fluid. The average absolute deviation is only 0.11% over the extremely large temperature range $0.6025 \leq T^* \leq 20$. If we translate this into real fluid terminology, we shall see that it is equivalent to $0.46 \leq T_r \leq 15$; for methane, this means $90 \leq T \leq 2900$ K (critical temperature for methane $T_c = 190.4$ K). Parameter values are given in Table 2.

One may note that the proposed equation does not satisfy the requirement of zero second virial coefficient at infinite temperature. However, none of the above mentioned expressions does and eqn. (14), which has only 5 terms, is still better than similar equations (inverse temperature series) which do not have a constant term, and thus do satisfy the infinite temperature limit, of up to nine terms. It must also be noted that at the extremely high temperatures involved, the first derivative of the second virial data is still positive; a maximum and, eventually, zero will be approached at much higher temperatures.

THE EQUATION OF STATE

The proposed equation of state for the Lennard-Jones fluid

The starting expression for developing our equation of state for the LJ fluid is a general form of eqn. (1):

$$z = \frac{f_1 + f_2 y + f_3 y^2 + f_4 y^3}{(1 + f_5 y)^3} \tag{15}$$

Preliminary calculations suggested that our objective stated in the Introduction could be met by setting $f_1 = 1$ and $f_5 = -1$ and making f_2, f_3 and f_4 functions of the reduced temperature. One may note that it is necessary to set $f_1 = 1$ so that the ideal gas limit ($z = 1$ at $y = 0$) is satisfied.

The f_2 values were first obtained directly from the second virial coefficient, since for the proposed equation

$$B_2^* = \tfrac{1}{4}(f_2 + 3) \tag{16}$$

Then, the corresponding expression for f_2 would be obtained using eqns. (14) and (16).

$$f_2 = 4\left(a + \frac{b}{\sqrt{T^*}} + \frac{c}{T^*} + \frac{d}{T^{*2}} + \frac{e}{T^{*3}}\right) - 3 \tag{17}$$

These f_2 values combined with f_3 and f_4 values obtained from VLE and supercritical PVT data led to an equation of state that, while giving an excellent representation of the pure LJ fluid phase envelope and the exact second virial coefficient, failed badly at high densities and in binary VLE predictions. Bryan and Prausnitz (1987) also had difficulties when they used the second virial coefficient in the development of their equation of state for dipolar hard spheres. They associated the problems in the estimation of high-density fluid (liquid or gas) properties with the slow convergence of the virial series at liquid-like densities.

Therefore it was decided to use subcooled liquid PVT and second virial (Barker et al., 1966) data, so that the LJ fluid behavior is correctly described at high densities and high temperatures, respectively. The following algorithm was used:
(a) At each temperature for which we have subcooled liquid data ($T^* = 0.720, 0.800, 0.810, 0.820, 0.902, 0.977, 1.060, 1.080, 1.135, 1.200, 1.235$), find a set of f_2, f_3 and f_4 so that eqn. (15) matches the subcooled liquid PVT behavior and satisfies the P_s^* and y_L calculated from eqns. (8) and (10), respectively; this was achieved as follows:
   (i)   Assume a value for f_2.
   (ii) Use the algorithm presented in the Appendix to find the f_3 and f_4 values that give correct vapor pressures and saturated liquid densities.
   (iii) Calculate the following objective function over the subcooled liquid range:

   $$Q = \sum (P_{\text{calc}} - P_{\text{exp}})^2 \tag{18}$$

   which represents the sum of the squares of differences between the calculated and the experimental pressures.
   (iv) Return to step (i), using a regression routine, and adjust the f_2 value until the objective function is minimized.
(b) Find the f_2 values from the experimental reduced second virial coefficient using eqn. (16).
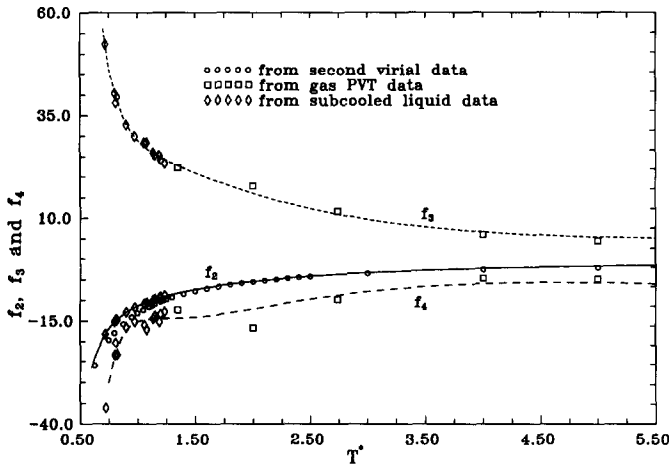
Fig. 1. f_i as a function of temperature: (———) f_2 correlation; (- - - - - -) f_3 correlation; (— — —) f_4 correlation; ($\Diamond\Diamond\Diamond\Diamond$) subcooled liquid *PVT* data; ($\Box\,\Box\,\Box\,\Box$) gas *PVT* data; ($\bigcirc\bigcirc\bigcirc\bigcirc$) second virial data.

(c) Correlate the f_2 values calculated in steps (a) and (b) with the reduced temperature weighting heavily data from step (a).

(d) For each temperature for which we have gas data ($T^* = 1.35$, 2.0, 2.74, 4.0 and 5.0), find f_3 and f_4 so that eqn. (15) matches the gas *PVT* behavior.

(e) Correlate the f_3 and f_4 values that were calculated in steps (a) and (d) with the reduced temperature; data from step (a) were heavily weighted in order to obtain successful VLE results.

Once the analytical expressions for the f_is were developed, the f_2 one was slightly adjusted to improve the final VLE results, as described in the Appendix.

TABLE 3

Parameter values in the expressions used for the calculation of f_2, f_3 and f_4 (eqn. (19))

Parameter	f_2	f_3	f_4
a	− 7.55136	61.4346	− 97.8311
b	42.35243	− 307.4431	470.7414
c	− 71.27149	459.8369	− 671.6129
d	38.42076	− 278.7989	425.8498
e	− 13.30967	94.0503	− 142.3163
Aver. abs. deviation (%)	0.1606	2.208	6.400
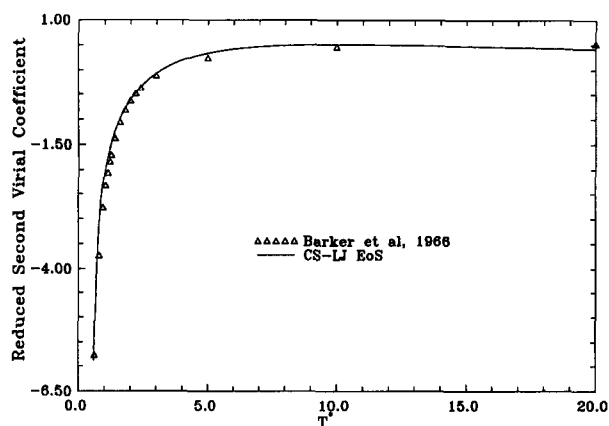
Fig. 2. Theoretical ($\triangle$ $\triangle$ $\triangle$ $\triangle$) and calculated from the CS–LJ EoS (———) reduced second virial coefficient of the LJ fluid.

The f_i values thus obtained from the previous algorithm are plotted versus T^* in Fig. 1. They were correlated with T^* using expressions similar to eqn. (14):

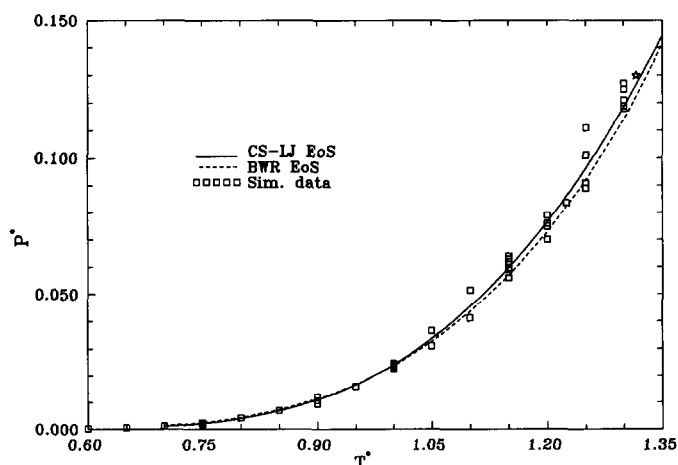$$f_i = a_i + \frac{b_i}{\sqrt{T^*}} + \frac{c_i}{T^*} + \frac{d_i}{T^{*2}} + \frac{e_i}{T^{*3}} \qquad (19)$$

Fig. 3. Vapor pressure predictions for the LJ fluid: ($\star$) critical point of the pure LJ fluid; ($\square$ $\square$ $\square$ $\square$) molecular simulation VLE data; (———) CS–LJ EoS; (- - - - - -) Nicolas et al. BWR EoS.
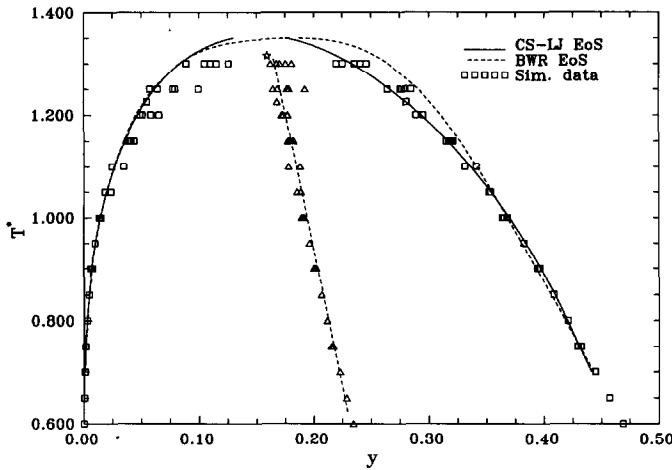
Fig. 4. Prediction of the phase envelope for the pure LJ fluid (T^* vs. y): symbols are the same as for Fig. 3; (- - △ - - △ - -) rectilinear diameter law.

The parameter values obtained are given in Table 3. The average absolute deviations were 0.16, 2.2 and 6.4% for f_2, f_3 and f_4, respectively. These correlations are shown graphically in Fig. 1. Equation (15) with $f_1 = 1$, $f_5 = -1$ and f_2, f_3 and f_4 as described previously represents the proposed Carnahan–Starling-type equation of state for the Lennard-Jones fluid, which is hereafter referred to as the CS–LJ EoS.
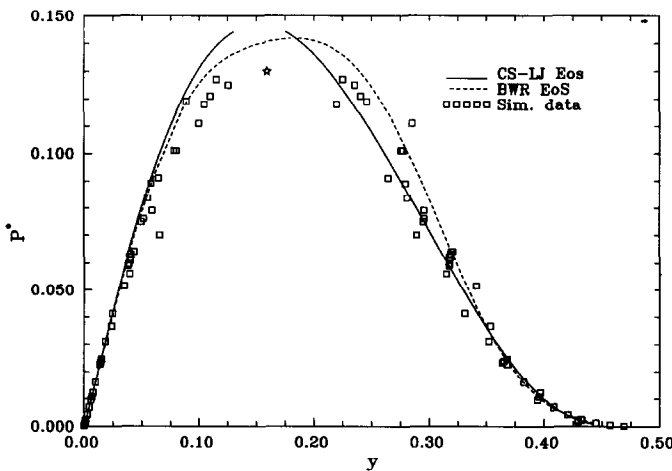
Fig. 5. Prediction of the phase envelope for the pure LJ fluid (P^* vs. y): symbols are the same as for Fig. 3.
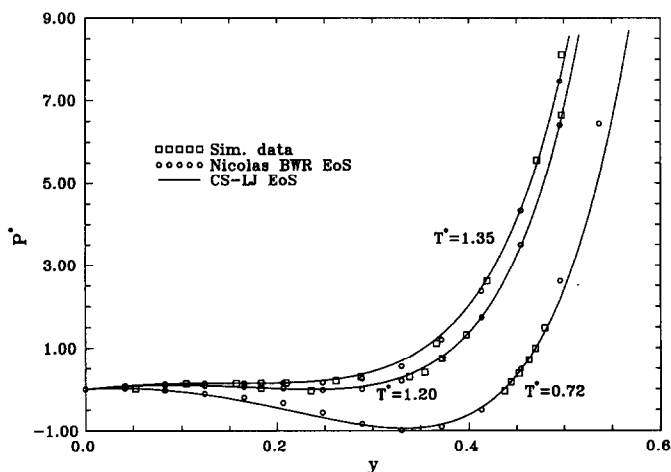
Fig. 6. *PVT* results (*P** vs. *y*) for the pure LJ fluid (*T** = 0.72, 1.20 and 1.35): (□ □ □ □) molecular simulation *PVT* data; (———) CS–LJ EoS; (○○○○) BWR EoS.

Pure fluid results

Predictions of the reduced second virial coefficients are presented in Fig. 2. Notice that satisfactory results are obtained even at the subcritical temperatures where the f_2 was obtained by heavily weighting the liquid *PVT* data.
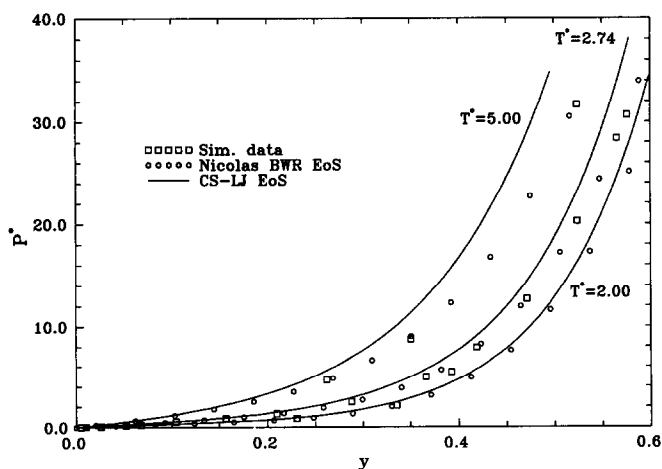

Fig. 7. *PVT* results (*P** vs. *y*) for the pure LJ fluid (*T** = 2.00, 2.74 and 5.00): symbols are the same as for Fig. 6.

VLE predictions of the proposed and Nicolas et al. EoS are presented in Figs. 3, 4 and 5. Excellent results are obtained, except in the critical region, as the proposed EoS does not reproduce the true critical point of the LJ fluid; the T_c^*, P_c^* and ρ_c^* values obtained are 1.355, 0.147 and 0.291, respectively. When the correct critical point was used in the development of the CS–LJ EoS, it was absolutely necessary to use discontinuous expressions for the description of f_i.

Typical PVT results are presented in Figs. 6 and 7. Satisfactory representation of the simulation data is obtained, except at the higher temperature and density values.

MIXTURES

Mixing and combining rules: systems studied

Harismiadis et al. (1991) have recently demonstrated that use of the simplest form of conformal solution theory, the van der Waals one fluid
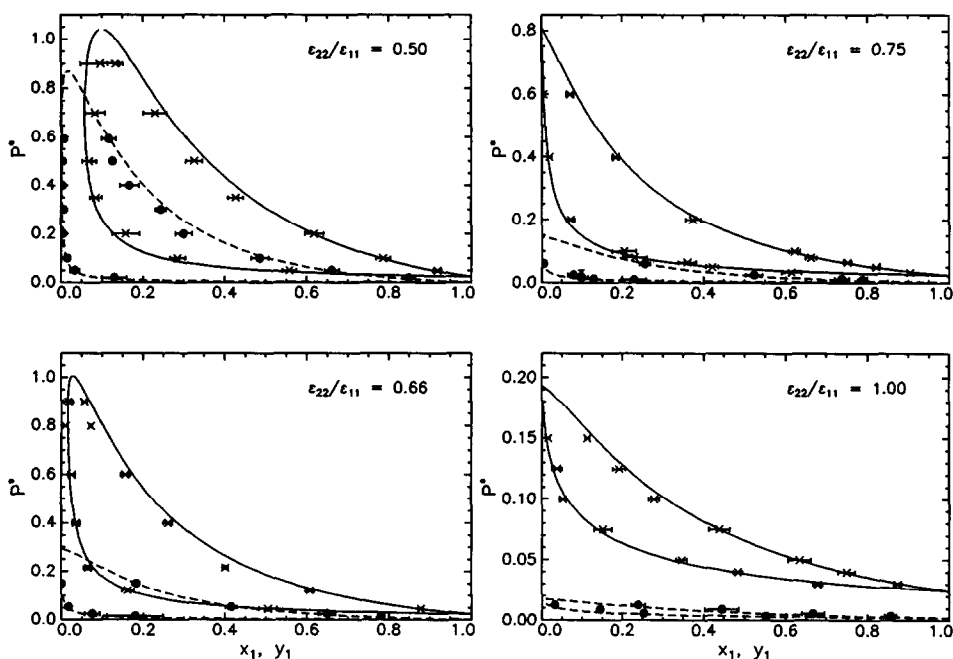

Fig. 8. Reduced pressure vs. mole fraction of the first component in liquid and vapor phases for the systems with $\sigma_{22}/\sigma_{11} = 0.5$. Monte Carlo results: ($\times$), $T^* = 1.00$; ($\bullet$), $T^* = 0.75$, Conformal solutions theory results: (————), $T^* = 1.00$; (— — — —), $T^* = 0.75$.

(vdW1f) approximation, in the Nicolas et al. BWR EoS for the LJ fluid provided successful prediction of their molecular simulation VLE results for the binary LJ fluid.

$$\sigma_{mix}^3 = \sum_i \sum_j z_i z_j \sigma_{ij}^3 \qquad \epsilon_{mix} = \frac{1}{\sigma_{mix}^3} \sum_i \sum_j z_i z_j \epsilon_{ij} \sigma_{ij}^3 \qquad (20)$$

For the potential parameters of the unlike molecular interactions, σ_{ij} and ϵ_{ij}, the Lorentz–Berthelot combining rules were used.

$$\sigma_{ij} = \frac{\sigma_{ii} + \sigma_{jj}}{2} \qquad \epsilon_{ij} = \sqrt{\epsilon_{ii}\epsilon_{jj}} \qquad (21)$$
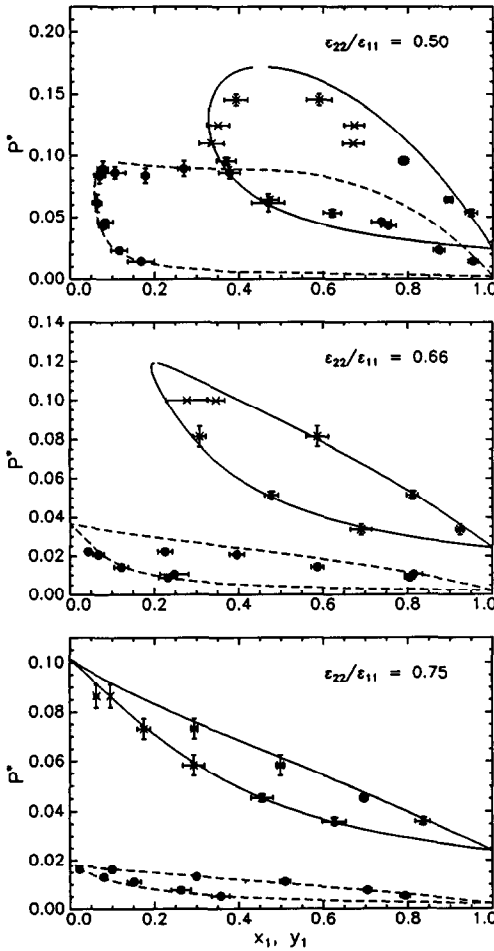

Fig. 9. Reduced pressure vs. mole fraction of the first component in liquid and vapor phases for the systems with $\sigma_{22}/\sigma_{11} = 1.0$; symbols are the same as for Fig. 8.

The performance of the proposed CS–LJ EoS was tested using also the vdW1f approximation against the same systems of Harismiadis et al., namely:

$\sigma_{22}/\sigma_{11} = 0.5$ and $\epsilon_{22}/\epsilon_{11} = 0.50$, 0.66, 0.75, 1.00

$\sigma_{22}/\sigma_{11} = 1.0$ and $\epsilon_{22}/\epsilon_{11} = 0.50$, 0.66, 0.75

$\sigma_{22}/\sigma_{11} = 1.5$ and $\epsilon_{22}/\epsilon_{11} = 0.66$, 0.75, 1.00

Binary mixture results

The binary mixture results of the proposed equation are presented in Figs. 8–13, as pressure–composition and pressure–density diagrams. Pres-
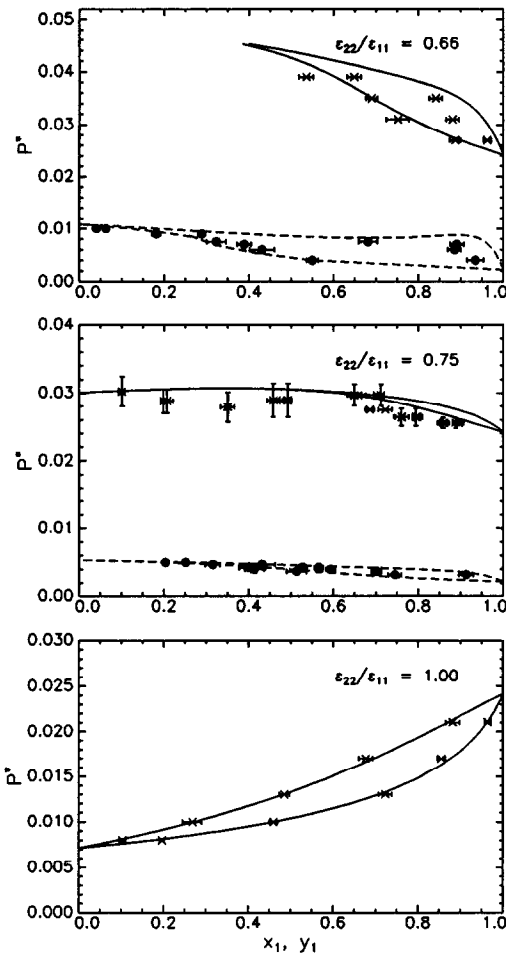

Fig. 10. Reduced pressure vs. mole fraction of the first component in liquid and vapor phases for the systems with $\sigma_{22}/\sigma_{11} = 1.5$; symbols are the same as for Fig. 8.
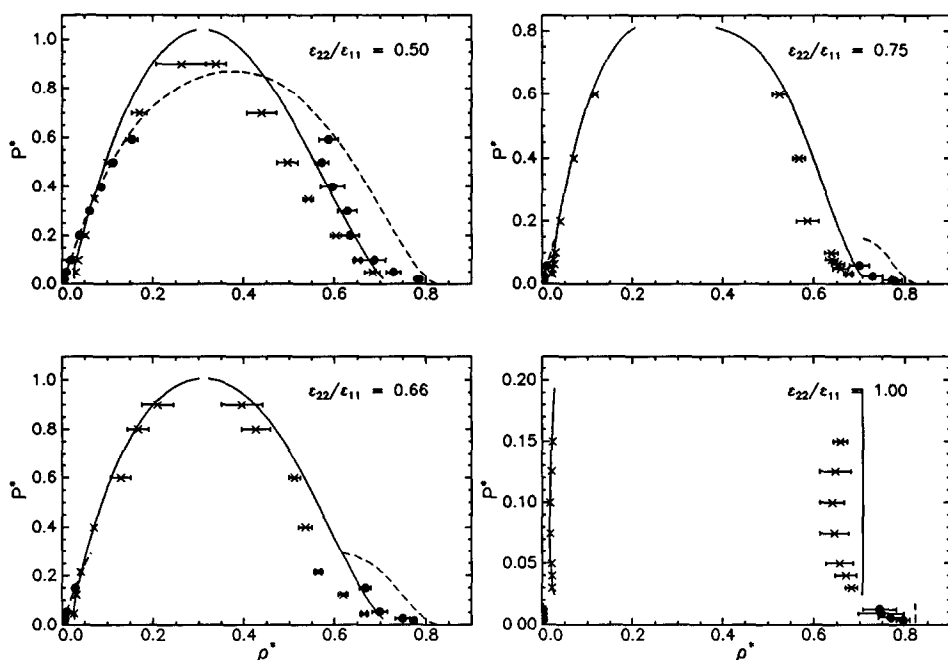
Fig. 11. Reduced pressure vs. reduced density in liquid and vapor phases for the systems with $\sigma_{22}/\sigma_{11} = 0.5$; symbols are the same as for Fig. 8.

sure and temperature are reduced with the first component's potential parameters, while density is reduced with the mixture's potential parameters.

The overall agreement between the Monte Carlo results and those obtained with the proposed CS–LJ EoS and the vdW1f theory for the pressure–composition diagrams (Figs. 8–10) is very satisfactory and similar to that obtained with the Nicolas et al. BWR EoS. In particular:

(i)   For $\sigma_{22}/\sigma_{11} = 0.5$ (Fig. 8), the whole representation is very good and the proposed equation is doing slightly better than the Nicolas et al. BWR EoS near the critical point for $\epsilon_{22}/\epsilon_{11} = 0.5$.

(ii) For $\sigma_{22}/\sigma_{11} = 1.0$ (Fig. 9), the results are similar to those obtained with the Nicolas et al. BWR EoS, except at the low $\epsilon_{22}/\epsilon_{11} = 0.5$ ratio, where the latter gives better but not completely satisfactory results. On the other hand, they are significantly better for all $\epsilon_{22}/\epsilon_{11}$ ratios than those obtained with the Adachi et al. version of the BWR EoS for·the LJ fluid that are reported by Harismiadis et al.

(iii) At $\sigma_{22}/\sigma_{11} = 1.5$ (Fig. 10), the results for $\epsilon_{22}/\epsilon_{11} = 1.0$ and 0.75 are similar to those with the Nicolas et al. BWR EoS, but inferior to them for the low $\epsilon_{22}/\epsilon_{11}$ ratio of 0.66.
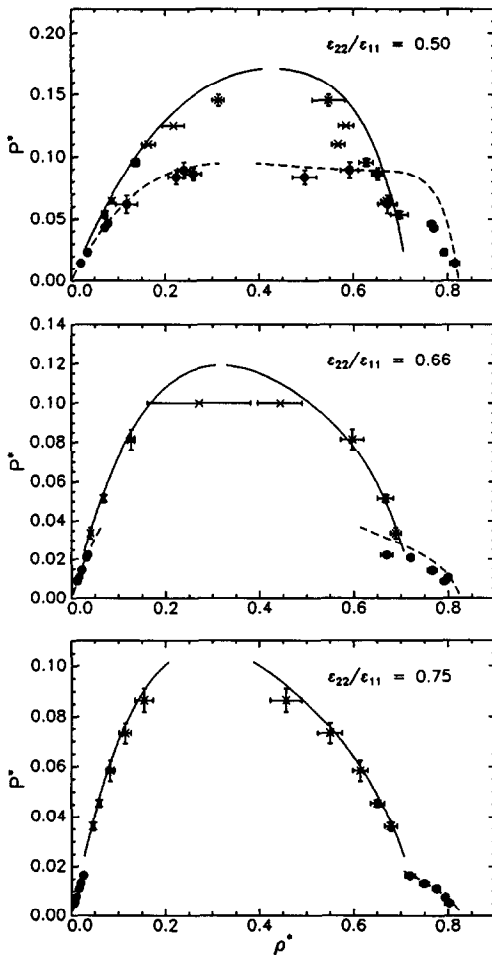
Fig. 12. Reduced pressure vs. reduced density in liquid and vapor phases for the systems with $\sigma_{22}/\sigma_{11} = 1.0$; symbols are the same as for Fig. 8.

Turning to the pressure–density results (Figs. 11–13) the agreement between the Monte Carlo results and those obtained with the proposed CS–LJ EoS and the vdW1f theory is less satisfactory. In particular:

(i)   For $\sigma_{22}/\sigma_{11} = 0.5$ (Fig. 11), there is a slight overestimation of the liquid densities at both temperatures. Compared with the Nicolas et al. BWR EoS, the results are much better for the prediction of liquid densities, while there is no noticeable difference in the quality of the vapor densities' predictions.

(ii) For $\sigma_{22}/\sigma_{11} = 1.0$ (Fig. 12), the results at $\epsilon_{22}/\epsilon_{11} = 0.75$ and 0.66 are somewhat better than those with the Nicolas et al. BWR EoS, but poorer for the low value of $\epsilon_{22}/\epsilon_{11} = 0.5$ and the low temperature.
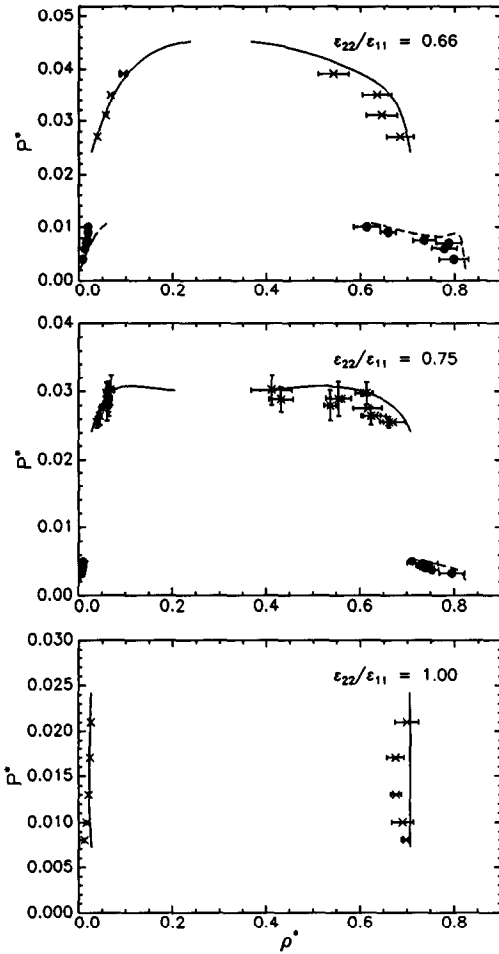
Fig. 13. Reduced pressure vs. reduced density in liquid and vapor phases for the systems with $\sigma_{22}/\sigma_{11} = 1.5$; symbols are the same as for Fig. 8.

(iii) For $\sigma_{22}/\sigma_{11} = 1.5$ (Fig. 13), while there is no significant difference between predicted and simulation results, the shape of the curves at $\epsilon_{22}/\epsilon_{11} = 0.75$ and $T^* = 1.0$ and at $\epsilon_{22}/\epsilon_{11} = 0.66$ and $T^* = 0.75$ is unsatisfactory. The Nicolas et al. BWR EoS results are similar, but do not have these problems.

DISCUSSION AND CONCLUSIONS

The proposed CS-type EoS gives very satisfactory results for the pure LJ fluid, especially considering its simplicity when compared with the BWR

TABLE 4

Critical properties of the LJ fluid

Source	T_c^*	P_c^*	ρ_c^*
Nicolas et al. BWR EoS	1.35	0.142	0.35
Adachi et al. BWR EoS	1.273	0.119	0.284
CS–LJ EoS	1.355	0.147	0.290
Molecular simulation	1.316 ± 0.006	0.13 ± 0.01	0.304 ± 0.006

one. There are some problems in the critical region because of the non-analytical nature of the critical point. Similar problems exist with the Nicolas et al. and the Adachi et al. versions of the BWR EoS since, as demonstrated in Table 4, they also do not predict the correct critical point.

Binary mixture results using the vdW1f theory are satisfactory. In general, they are comparable with those of the Nicolas et al. BWR EoS, and superior to those of the Adachi et al. BWR EoS. In the rather unreal, from the practical point of view, cases where $\sigma_{22} > \sigma_{11}$ and $\epsilon_{22} < \epsilon_{11}$, they are somewhat inferior to those of the Nicolas et al. BWR, but still superior to those of the Adachi et al. BWR.

A comparison of the results obtained by the two BWR EoS and the CS–LJ EoS in describing the simulation data tends to support the conclusion reached by Harismiadis et al. that whatever differences exist between the vdW1f theory and simulation are probably due to the EoS itself and not the theory. Considering in addition the fact that, in terms of pure component VLE predictions a main difference among the three EoS is in the critical point that they predict, it is apparent that improvement in the critical region is needed before a conclusive comparison between the vdW1f theory and molecular simulation can be made.

It appears, in conclusion, that for theoretical work, such as testing the vdW1f theory, a better EoS for the LJ fluid is needed. On the other hand, considering the excellent results obtained with the CS–LJ EoS for systems of practical importance, where σ_{22}/σ_{11} and $\epsilon_{22}/\epsilon_{11}$ are both greater or both smaller than 1.0, it is expected that the proposed EoS would be a suitable reference term for the development of equations of state for real systems.

LIST OF SYMBOLS

B_n^* reduced nth virial coefficient of the LJ fluid ($n = 2,3,\dots$)
P^* reduced pressure for the LJ fluid, defined as $P^* = P\sigma^3/\epsilon$
P_c^* reduced critical pressure for the LJ fluid
P_s^* reduced vapor pressure for the LJ fluid (obtained from molecular simulation)
r intermolecular distance
T^* reduced temperature for the LJ fluid, defined as $T^* = kT/\epsilon$
T_c^* reduced critical temperature for the LJ fluid
U_{ij} intermolecular potential
x_i molar fraction of species i in a given liquid mixture
y density, defined as $y = \pi\rho^*/6$
y_c critical density, defined as $y = \pi\rho_c^*/6$
y_i molar fraction of species i in a given vapor mixture
y_L saturated liquid density, defined as $y_L = \pi\rho_L^*/6$
y_V saturated vapor density, defined as $y_V = \pi\rho_V^*/6$
z compressibility factor, defined as $z = P^*/(\rho^* T^*)$
z_i molar fraction of species i in a given mixture

Greek letters

ϵ_{ii} LJ energy potential parameter for species i
ϵ_{ij} LJ energy potential parameter for unlike molecular interactions (defined by the combining rules)
ϵ_{mix} LJ energy potential parameter for mixtures (defined by the mixing rules)
ρ number density, defined as $\rho = N/V$ (molecules per cubic meter)
ρ^* reduced density for the LJ fluid, defined as $\rho^* = \rho\sigma^3$
ρ_c^* reduced critical density for the LJ fluid
ρ_L^* reduced saturated liquid density for the LJ fluid (obtained from molecular simulation)
ρ_V^* reduced saturated vapor density for the LJ fluid (obtained from molecular simulation)
σ_{ii} LJ size potential parameter for species i
σ_{ij} LJ size potential parameter for unlike molecular interactions (defined by the combining rules)
σ_{mix} LJ size potential parameter for mixtures (defined by the mixing rules)

REFERENCES

Abbott, M.M., 1973. Cubic equations of state. AIChE J., 19 (3): 596–601.
Adachi, Y., Fijihara, I., Takamiya, M. and Nakanishi, K., 1988. Generalized equation of state for Lennard-Jones fluids. I. Pure fluids and simple mixtures. Fluid Phase Equilibria, 39: 1–38.
Adams, D.J., 1976. Calculating the low temperature vapor line by Monte Carlo. Mol. Phys., 32 (3): 647–657.
Adams, D.J., 1979. Calculating the high-temperature vapor line by Monte Carlo. Mol. Phys., 37 (1): 211–221.
Barker, J.A., Leonard, P.J. and Pompe, A., 1966. Fifth virial coefficients. J. Chem. Phys., 44(11): 4206–4211.
Bryan, P.F. and Prausnitz, J.M., 1987. Thermodynamic properties of polar fluids from a perturbed-dipolar-hard-sphere equation of state. Fluid Phase Equilibria, 38: 201–216.
Carnahan, N.F. and Starling, K.E., 1969. Equation of state for nonattracting rigid spheres. J. Chem. Phys., 51 (2): 635–636.
Daubert, T.E. and Danner, R.D., 1989. Data Compilation Tables of Properties of Pure Compounds. AIChE, NY.
Hansen, J.P. and Verlet, L., 1969. Phase transitions of the Lennard-Jones systems. Phys. Rev., 184 (1): 151–161.
Harismiadis, V.I., Koutras, N.K., Tassios, D.P. and Panagiotopoulos, A.Z., 1991. How good is conformal solutions theory for phase equilibrium predictions? Gibbs ensemble simulations of binary Lennard-Jones mixtures. Fluid Phase Equilibria, 65: 1–18.
Nicolas, J.J., Gubbins, K.E., Streett, W.B. and Tildesley, D.J., 1979. Equation of state for the Lennard-Jones fluid. Mol. Phys., 37 (5): 1429–1454.
Panagiotopoulos, A.Z., 1987. Direct determination of phase coexistence properties of fluids by Monte Carlo simulation in a new ensemble. Mol. Phys., 61 (4): 813–826.
Panagiotopoulos, A.Z., 1991. Personal communication.
Panagiotopoulos, A.Z. Quirke, N., Stapleton, M. and Tildesley, D., 1988. Phase equilibria by simulation in the Gibbs ensemble. Alternative derivation, generalization and application to mixture and membrane equilibria. Mol. Phys., 63 (4): 527–545.
Perry, R.H. and Green, D., 1984. Perry's Chemical Engineers' Handbook, 6th edn. McGraw-Hill, New York.
Reid, R.C., Prausnitz, J.M. and Poling, B.E., 1987. The Properties of Gases and Liquids, 4th edn. McGraw-Hill, New York.
Rushbrooke, G.S., Stell, G. and Høye, J.S., 1973. Theory of polar fluids I. Dipolar hard spheres. Mol. Phys., 26: 1199–1215.
Smit, B., 1990. Simulation of phase coexistence: from atoms to surfactants. PhD dissertation, Utrecht University.
Smit, B. and Frenkel, D., 1989. Calculation of the chemical potential in the Gibbs ensemble. Mol. Phys., 68 (4): 951–958.
Tsonopoulos, C., 1974. An empirical correlation of second virial coefficients. AIChE J., 20 (2): 263–272.

APPENDIX

The fugacity coefficient of the pure LJ fluid

The fugacity coefficient for a pure fluid is obtained from the equation (Reid et al., 1987):

$$\ln \phi = z - 1 - \ln z - \frac{1}{RT} \int_{\infty}^{V} \left(P - \frac{RT}{V} \right) dV \tag{A1}$$

where V is the molar volume, T the absolute temperature, P the pressure and z the compressibility factor. For the CS–LJ EoS (eqn. (15) with $f_1 = 1$, $f_5 = -1$ and f_2, f_3 and f_4 given by eqn. (19) using the parameter values presented in Table 3), noting that:

$$y = \frac{(\pi/6)\sigma^3 N_A}{V} \qquad z = \frac{P^*}{(6/\pi)yT^*} \tag{A2}$$

where N_A is the Avogadro number, we obtain, after some manipulation, the fugacity coefficient of the pure LJ fluid:

$$\ln \phi = z - \ln z - 1 - (1 + f_4) \ln(1 - y) + (1 - f_3 - 2f_4)\left(\frac{y}{1 - y}\right)$$

$$+ \tfrac{1}{2}(1 + f_2 + f_3 + f_4)\left(\frac{2y - y^2}{(1 - y)^2}\right) \tag{A3}$$

From the equality of fugacities we have

$$f^L = f^V \Leftrightarrow \ln \phi^V = \ln \phi^L \tag{A4}$$

where the superscripts L and V denote the liquid and the vapor phase, respectively.

Evaluation of f_3 and f_4 (when f_2 is known) at a given temperature from the corresponding vapor pressures and saturated liquid densities of the pure LJ fluid

Substitution of eqn. (A3) into eqn. (A4) yields:

$$P_s^* \frac{\pi\left(\dfrac{1}{y_L} - \dfrac{1}{y_V}\right)}{6T^*} = -(1 + f_4)\ln\frac{1 - y_V}{1 - y_L} + \ln\frac{y_V}{y_L}$$

$$+ (1 - f_3 - 2f_4)\left(\frac{1}{1 - y_V} - \frac{1}{1 - y_L}\right)$$

$$+ \tfrac{1}{2}(1 + f_2 + f_3 + f_4)\left(\frac{1}{(1 - y_V)^2} - \frac{1}{(1 - y_L)^2}\right) \tag{A5}$$

where y_V and y_L are calculated by solving the following quartic equation obtained from the proposed equation of state:

$$(6f_4T^*)y^4 + (6f_3T^* - \pi P^*)y^3 + (6f_2T^* - 3\pi P^*)y^2$$
$$+ (6T^* + 3\pi P^*)y - (\pi P^*) = 0 \tag{A6}$$

Our next equation is obtained by requiring that the CS–LJ EoS is satisfied for the known vapor pressure and saturated liquid density values:

$$z_L = \frac{\pi P_s^*}{6y_L T^*} = \frac{1 + f_2 y_L + f_3 y_L^2 + f_4 y_L^3}{(1 - y_L)^3} \tag{A7}$$

Thus we have to solve a system of three equations ((A5), (A6) and (A7)) with three unknowns (f_3, f_4 and y_V). The following iterative procedure was used:

(i) For a given temperature (T^*), find the vapor pressure (P_s^*) and the saturated liquid density (y_L) values using eqns. (8) and (10), respectively, and Table 2. The f_2 value is assumed to be known.

(ii) Assume an initial value for f_4.

(iii) Calculate f_3 from eqn. (A7).

(iv) Solve eqn. (A6) for y_V.

(v) Solve eqn. (A5) for f_4.

(vi) Return to step (iii), unless the f_4 value just calculated is sufficiently close to its previous estimate.

We note that:

(i) A satisfactory, in most cases, initial value for f_4 was found by demanding our equation to satisfy the experimental vapor pressure for both y_L and y_V:

$$f_4 = \frac{\pi P_s^*}{6T^*(y_L - y_V)}$$
$$\times \left(\frac{(1-y_L)^3 - y_L(1+f_2 y_L)}{y_L^3} - \frac{(1-y_V)^3 - y_V(1+f_2 y_V)}{y_V^3} \right) \tag{A8}$$

(ii) Equations (A5) and (A7) are linear in f_3 and f_4; yet, the system that must be solved is not, because y_V is calculated from eqn. (A6).

(iii) From eqn. (A6) we are here interested in the y_V value only; step (iii) of the algorithm assures that the y_L value that could be calculated would be equal to the experimental one. To find the saturated vapor density (y_V), eqn. (A6) could be solved by using any simple iterative approach (e.g. direct substitution); one has only to remark that this quantity is very small and its square and cube diminish.

Evaluation of f_2 at a given temperature from the corresponding vapor pressure of the pure LJ fluid

It can easily be seen that, for a given set of T^*, P_s^*, f_3 and f_4, the f_2 value is calculated in a unique way. The following iterative procedure was used:

(i)   For a given temperature (T^*), calculate the vapor pressure (P_s^*) and the f_3 and f_4 values using eqns. (8) and (10), respectively, and Table 2.

(ii) Assume an initial value for f_2.

(iii) Solve eqn. (A6) for y_V and y_L.

(iv) Solve eqn. (A5) for f_2.

(v)   Return to step (iii), unless the f_2 value just calculated is sufficiently close to its previous estimate.

Vapor–liquid equilibria calculations for the pure LJ fluid

To calculate the pure LJ fluid vapor pressure at a given temperature, the following steps are required:

(i)   Calculate the f_i using eqn. (19) and Table 3.

(ii) Solve eqn. (A6) for both y_L and y_V.

(iii) Substitute y_L and y_V in eqn. (A5).

(iv) Solve eqn. (A5) for P_s^*.

For the purposes of our work, since pure fluid vapor pressure and saturated liquid and vapor density calculations demand eqn. (A6) to be solved for both y_L and y_V, a computer subroutine that solves quartic equations analytically was developed, extensively tested and applied. The algorithm is given by Perry and Green (1984). In order to obtain phase equilibria, eqn. (A6) should have four real roots, one of which would be extremely large and considered useless. In fact, in solving eqn. (A6), y_L and y_V are, respectively, the smallest and largest positive roots that are less than 0.5.

Expressions for the fugacity coefficients of the mixture components

The fugacity coefficient of the component i of a mixture is given by

$$\ln \hat{\phi}_i = z - 1 - \ln z - \int_\infty^V \left[\left(\frac{\partial(nz)}{\partial n_i} \right)_{T,V,n_{j \neq i}} - 1 \right] \frac{\mathrm{d}V}{V} \tag{A9}$$

where n is the total number of moles in the mixtures and n_i is the number of moles of component i.

Changing the integrating variable from V to y through eqn. (A2) we have

$$\ln \hat{\phi}_i = z - 1 - \ln z + \int_0^y \left(\frac{\partial (nz)}{\partial n_i} \right)_{T,\rho,n_{j\neq i}} \frac{dy}{y} - \int_0^y \frac{dy}{y} \tag{A10}$$

To evaluate the two integrals we note that

$$\int_0^y \left(\frac{\partial (nz)}{\partial n_i} \right)_{T,\rho,n_{j\neq i}} \frac{dy}{y} - \int_0^y \frac{dy}{y}$$

$$= \int_0^y \frac{z}{y} dy + \int_0^y \frac{n}{y} \frac{\partial z}{\partial y} \frac{\partial y}{\partial n_i} dy$$

$$+ \sum_{m=2}^4 \left(\int_0^y \frac{\partial z}{\partial f_m} \frac{\partial f_m}{\partial T^*} \frac{\partial T^*}{\partial n_i} \frac{n}{y} dy \right) - \int_0^y \frac{dy}{y} \tag{A11}$$

where

$$\int_0^y \frac{z}{y} dy = \int_0^y \frac{dy}{y} - (1 + f_4) \ln(1 - y)$$

$$+ \frac{1 - f_3 - 2f_4}{(1-y)} + \frac{1 + f_2 + f_3 + f_4}{2(1-y)^2} - \frac{3 + f_2 - f_3 - 3f_4}{2} \tag{A12}$$

$$\int_0^y \frac{n}{y} \frac{\partial z}{\partial y} \frac{\partial y}{\partial n_i} dy$$

$$= \frac{2}{\sigma_{mix}^3} \left(\sum_k z_k \sigma_{ki}^3 - \sigma_{mix}^3 \right)$$

$$\times \left((1 + 2f_2 + f_4) + \frac{y^2(f_3 + 3f_4) + y(f_2 - 3f_4) + (1 + f_4)}{(1-y)^3} \right) \tag{A13}$$

$$\int_0^y \frac{\partial z}{\partial f_2} \frac{\partial f_2}{\partial T^*} \frac{\partial T^*}{\partial n_i} \frac{n}{y} dy = \frac{\partial f_2}{\partial T^*} \frac{\partial T^*}{\partial n_i} n \left(\frac{1}{2(1-y)^2} - \frac{1}{2} \right) \tag{A14}$$

$$\int_0^y \frac{\partial z}{\partial f_3} \frac{\partial f_3}{\partial T^*} \frac{\partial T^*}{\partial n_i} \frac{n}{y} dy = \frac{\partial f_3}{\partial T^*} \frac{\partial T^*}{\partial n_i} n \left(\frac{1}{2(1-y)^2} - \frac{1}{1-y} + \frac{1}{2} \right) \tag{A15}$$

$$\int_0^y \frac{\partial z}{\partial f_4} \frac{\partial f_4}{\partial T^*} \frac{\partial T^*}{\partial n_i} \frac{n}{y} dy = \frac{\partial f_4}{\partial T^*} \frac{\partial T^*}{\partial n_i} n \left(\frac{3}{2} - \ln(1-y) + \frac{1}{2(1-y)^2} - \frac{2}{1-y} \right)$$

$$\tag{A16}$$

$$\frac{\partial f_m}{\partial T^*} = -\frac{1}{2} b_m T^{-3/2} - c_m T^{-2} - 2 d_m T^{-3} - 3 e_m T^{-4} \tag{A17}$$

$$\frac{\partial T^*}{\partial n_i} = \frac{2}{n} T^* \frac{\epsilon_{\text{mix}} \sum_k z_k \sigma_{ki}^3 - \sum_k z_k \epsilon_{ki} \sigma_{ki}^3}{\epsilon_{\text{mix}} \sigma_{\text{mix}}^3} \tag{A18}$$

The values of b_m, c_m, d_m, e_m ($m = 2, 3, 4$) of eqn. (A17) are presented in Table 3.